

Study on stress fields in a V-Shape notched disk under distributed load.

Samadder LITON KUMAR*, Yoshio ARAI**, Eiichiro TSUCHIDA**

A new method is developed for determining the stress and displacement fields around a sharp V-shape notched disk which is symmetrically loaded on the circumferential edge. Complex eigen function expansion is used to satisfy the stress free condition of the sharp V-shape notch. Boundary condition of the external load applied on the circumferential edge is satisfied with the aid of the Schmidt method. An example of numerical calculation on the stress field is presented and examined. Approximation expressions based on the eigen function expansion are proposed and its validity is confirmed. Finally, the numerical results are compared to photoelastic experiment.

Key words: Eigenvalues, Photoelastic, Stress Singularity, Schmidt method, V-shape notch.

1. Introduction

Sharp corners are often found in welded joints, microelectronic chips, etc. and its structural integrity has recently become increasingly important. Williams⁽¹⁾ analyzed wedge with variety of edge boundary conditions. He noted that a power stress singularity ($\sigma_{ij} \propto Kr^{\lambda-1}$) can exist at the apex of the wedge. He also noticed that an arbitrary loading along the circumferential boundary can be formed by a linear combination of the eigen functions. Many studies have been done on the stress singularity and stress intensity factor of the V-shape notch⁽²⁻⁸⁾. The singular term describe the stress field just ahead of the apex of the notch. When the notch opening angle is large the singularity is not strong and the higher order terms of the eigen functions are necessary for precise expression of the stress field around the notch.

In this paper, Papkovitch-Neuber displacement potentials are used to determine the stresses and displacement equations. A new analytical method is developed to calculate the stress and displacement around a sharp V-shape notch in homogeneous elastic disk which is symmetrically loaded. Numerical calculations are carried out when the external loads are applied to the circumferential edge of the disk. The external boundary load condition are satisfied with the help of the Schmidt method. Approximation expressions based on the eigen function expansion are proposed and its validity is confirmed. Finally, the numerical results are compared to

photoelastic experiment.

2. Method of Solution

Consider V-shape notched disk subjected to extension in its plane. The opening angle of the notch is $2(\pi - b)$. Let the origin of coordinates be at the center of the circular plate and the relation of the Cartesian and polar system by $x = r \cos \theta, y = r \sin \theta$ and the radius of the disk is a . Based on the Papkovitch-Neuber potentials formulation, φ_0, φ_1 and the radial and tangential displacement components, u_r, u_θ , are given as follows⁽⁹⁾:

$$\left. \begin{aligned} 2Gu_r &= \frac{\partial \varphi_0}{\partial r} + r \cos \theta \frac{\partial \varphi_1}{\partial r} - \kappa \cos \theta \varphi_1, \\ 2Gu_\theta &= \frac{1}{r} \frac{\partial \varphi_0}{\partial \theta} + \cos \theta \frac{\partial \varphi_1}{\partial \theta} + \kappa \sin \theta \varphi_1, \end{aligned} \right\} \quad (1)$$

where, $\nabla^2 \varphi_0 = \nabla^2 \varphi_1 = 0$ and κ is defined as follows:

$$\kappa = \begin{cases} \frac{3 - \nu}{1 + \nu} & \text{(plane stress),} \\ \frac{3 - 4\nu}{3 - 4\nu} & \text{(plane strain),} \end{cases}$$

where, ν is Poisson's ratio, G is shear modulus. The boundary conditions of this problem are

$$\left. \begin{aligned} (\sigma_\theta)_{\theta=\pm b} &= (\tau_{r\theta})_{\theta=\pm b} = 0, \\ (\sigma_r)_{r=a} &= p_o \bar{\sigma}_r(\theta), \\ (\tau_{r\theta})_{r=a} &= p_o \bar{\tau}_{r\theta}(\theta). \end{aligned} \right\} \quad (2)$$

Among the boundary conditions, the first boundary condition is the stress free boundary condition of

*Graduate Student of Saitama University
 **Department of Mechanical Engineering, Saitama University
 255 Shimo-Okubo, Sakura-Ku, Saitama-Shi, Japan.

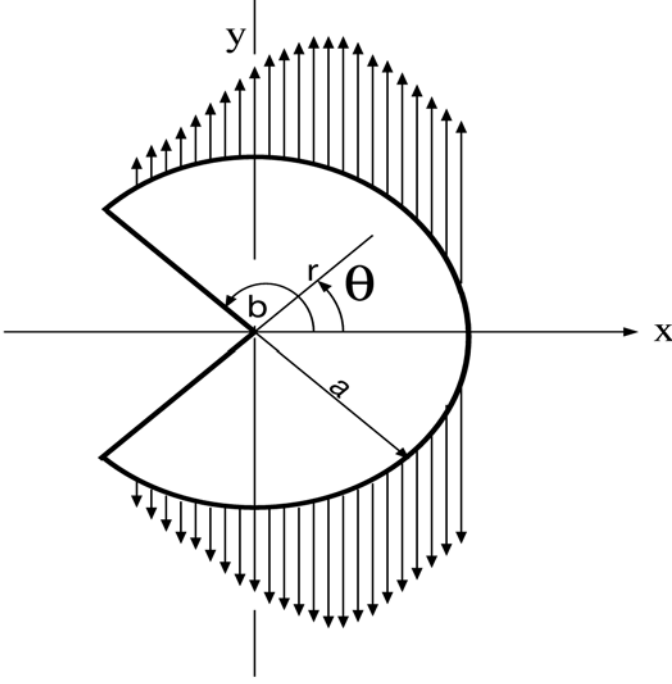


Figure 1: Circular plate subjected to distributed load on the circumferential edge

the notch and the second and third boundary conditions are external load on the circumferential edge defined as follows:

$$\left. \begin{aligned} \sigma_r(\theta) &= \frac{1}{2}(1 - \cos 2\theta) \cos \frac{\pi\theta}{2b}, \\ \tau_{r\theta}(\theta) &= \frac{1}{2} \sin 2\theta \cos \frac{\pi\theta}{2b}. \end{aligned} \right\} \quad (3)$$

Displacement potential function, φ_0, φ_1 , are expressed into harmonic function in polar co-ordinate,

$$\left. \begin{aligned} \varphi_0 &= p_0 \sum_{n=0}^{\infty} r^{\lambda_n+1} A_n \cos(\lambda_n + 1)\theta, \\ \varphi_1 &= p_0 \sum_{n=0}^{\infty} r^{\lambda_n} B_n \cos \lambda_n \theta, \end{aligned} \right\} \quad (4)$$

where, λ_n, A_n, B_n are the eigenvalues and the unknown constants respectively to be determined from boundary conditions. The equation of the stress and displacement fields have been developed using Eq.(1) and Eq.(4) .

$$\begin{aligned} \sigma_r &= p_0 \sum_{n=0}^{\infty} \lambda_n r^{\lambda_n-1} [A_n(\lambda_n + 1) \cos(\lambda_n + 1)\theta \\ &\quad + B_n \left\{ \frac{\lambda_n - \kappa}{2} \cos(\lambda_n + 1)\theta \right. \\ &\quad \left. + \frac{\lambda_n - 3}{2} \cos(\lambda_n - 1)\theta \right\}], \end{aligned} \quad (5)$$

$$\begin{aligned} \sigma_\theta &= -p_0 \sum_{n=0}^{\infty} \lambda_n r^{\lambda_n-1} [A_n(\lambda_n + 1) \cos(\lambda_n + 1)\theta \\ &\quad + B_n \left\{ \frac{\lambda_n - \kappa}{2} \cos(\lambda_n + 1)\theta \right. \\ &\quad \left. + \frac{\lambda_n + 1}{2} \cos(\lambda_n - 1)\theta \right\}], \end{aligned} \quad (6)$$

$$\begin{aligned} \tau_{r\theta} &= -p_0 \sum_{n=0}^{\infty} \lambda_n r^{\lambda_n-1} [A_n(\lambda_n + 1) \sin(\lambda_n + 1)\theta \\ &\quad + B_n \left\{ \frac{\lambda_n - \kappa}{2} \sin(\lambda_n + 1)\theta \right. \\ &\quad \left. + \frac{\lambda_n - 1}{2} \sin(\lambda_n - 1)\theta \right\}], \end{aligned} \quad (7)$$

$$\begin{aligned} 2Gu_r &= p_0 \sum_{n=0}^{\infty} r^{\lambda_n} [A_n(\lambda_n + 1) \cos(\lambda_n + 1)\theta \\ &\quad + B_n \frac{\lambda_n - \kappa}{2} \{ \cos(\lambda_n + 1)\theta \\ &\quad + \cos(\lambda_n - 1)\theta \}], \end{aligned} \quad (8)$$

$$\begin{aligned} 2Gu_\theta &= -p_0 \sum_{n=0}^{\infty} r^{\lambda_n} [A_n(\lambda_n + 1) \sin(\lambda_n + 1)\theta \\ &\quad + B_n \left\{ \frac{\lambda_n - \kappa}{2} \sin(\lambda_n + 1)\theta \right. \\ &\quad \left. + \frac{\lambda_n + \kappa}{2} \sin(\lambda_n - 1)\theta \right\}]. \end{aligned} \quad (9)$$

By using the stress free boundary condition, the characteristic equation can be expressed into following forms:

$$\lambda_n^2(\lambda_n + 1)(\lambda_n \sin 2b + \sin 2\lambda_n b) = 0. \quad (10)$$

The relationship between unknown constants A_n and B_n can also be expressed into following forms;

$$\begin{aligned} B_n &= -2(\lambda_n + 1) \cos(\lambda_n + 1)b A_n \\ &\quad / \{ (\lambda_n - \kappa) \cos(\lambda_n + 1)b \\ &\quad + (\lambda_n + 1) \cos(\lambda_n - 1)b \}. \end{aligned} \quad (11)$$

For calculating eigenvalues the characteristic equation is solved by using the Newton-Raphson method. To satisfy the boundary conditions of the circumferential edge, the Schmidt method is used⁽¹⁰⁾. The calculated stresses can be expressed into complex form as follows:

$$(\sigma_r + i\tau_{r\theta})_{r=a} = p_0 \sum_{n=0}^{\infty} A_n W_n(\theta), \quad (12)$$

where, $W_n(\theta) = W_{rn} + iW_{\theta n}$, $i = \sqrt{-1}$,

$$\left. \begin{aligned} W_{rn} &= \lambda_n [(\lambda_n + 1) \cos(\lambda_n + 1)\theta \\ &\quad + R_n \left\{ \frac{\lambda_n - \kappa}{2} \cos(\lambda_n + 1)\theta \right. \\ &\quad \left. + \frac{\lambda_n - 3}{2} \cos(\lambda_n - 1)\theta \right\}], \\ W_{\theta n} &= -\lambda_n [(\lambda_n + 1) \sin(\lambda_n + 1)\theta \\ &\quad + R_n \left\{ \frac{\lambda_n - \kappa}{2} \sin(\lambda_n + 1)\theta \right. \\ &\quad \left. + \frac{\lambda_n - 1}{2} \sin(\lambda_n - 1)\theta \right\}], \end{aligned} \right\}$$

$$\begin{aligned} R_n &= -2(\lambda_n + 1) \cos(\lambda_n + 1)b A_n \\ &\quad / \{ (\lambda_n - \kappa) \cos(\lambda_n + 1)b \\ &\quad + (\lambda_n + 1) \cos(\lambda_n - 1)b \}. \end{aligned}$$

$W_n(\theta)$ can be expanded into an orthogonal function series $S_0, S_1, S_2, \dots, S_n$. External load can also be expanded into the orthogonal function series and we

get the following relationship;

$$\begin{aligned} (\bar{\sigma}_r + i\bar{\tau}_{r\theta})_{r=a} &= p_o \sum_{m=0}^{\infty} L_m S_m(\theta) \\ &= p_o \sum_{n=0}^{\infty} A_n W_n(\theta), \end{aligned} \quad (13)$$

where, $S_m(\theta)$ can also be expressed by series of $W_l(\theta)$ and the equation can be expressed by following forms;

$$S_m(\theta) = \sum_{l=0}^m \frac{M_{lm}}{M_{mm}} W_l(\theta), \quad (14)$$

$$L_i = \frac{\int_{-b}^b (\bar{\sigma}_r(\theta) + i\bar{\tau}_{r\theta}(\theta)) \bar{S}_i d\theta}{I_i},$$

$$I_i = \int_{-b}^b S_i \bar{S}_i d\theta.$$

M_{lm} is the minor of the element $d_{(l+1)(m+1)}$ in the matrix d_{np} .

$$d_{np} = \int_{-b}^b W_n, \bar{W}_p d\theta (n, p = 1, 2, 3 \dots m). \quad (15)$$

\bar{W}_p is defined as complex conjugate of W_p . From Eq.(15) and the boundary condition, Eq.(14), we can get

$$\sum_{n=0}^{\infty} A_n W_n(\theta) = \sum_{m=0}^{\infty} L_m \sum_{l=0}^m \alpha_{ml} W_l(\theta), \quad (16)$$

where, $\alpha_{ml} = \frac{M_{lm}}{M_{mm}}$. We can rewrite the right side of this equation as,

$$\begin{aligned} &\sum_{m=0}^{\infty} L_m \sum_{l=0}^m \alpha_{ml} W_l(\theta) \\ &= \sum_{m=0}^{\infty} \sum_{n=m}^{\infty} L_m \alpha_{nm} W_m(\theta). \end{aligned} \quad (17)$$

From equation (16) and (17) the unknown constants, A_n , can be expressed into following equation;

$$A_n = \sum_{m=n}^{\infty} L_m \alpha_{mn}. \quad (18)$$

Table1: Calculated eigenvalues, λ_n for k=9

$\lambda_0 = 0.5444837367$
$\lambda_1 = (1.6292573767, 0.2312505471)$
$\lambda_2 = (2.9718437731, 0.3739312054)$
$\lambda_3 = (4.3103772915, 0.4554935790)$
$\lambda_4 = (5.6471117736, 0.513683812)$
$\lambda_5 = (6.9828704415, 0.559108261)$
$\lambda_6 = (8.3180336878, 0.5964194271)$
$\lambda_7 = (9.6528039491, 0.6280993597)$
$\lambda_8 = (10.9872997833, 0.6556354568)$
$\lambda_9 = (12.3215956354, 0.6799917174)$

Table2: Calculated A_n for k=9

$A_0 = (-0.43874054, -3.8344519 \times 10^{-18})$
$A_1 = (-4.6860928 \times 10^{-2}, -6.30572053 \times 10^{-18})$
$A_2 = (-2.029204 \times 10^{-3}, -4.7431015 \times 10^{-18})$
$A_3 = (4.166764 \times 10^{-4}, -7.2929320 \times 10^{-19})$
$A_4 = (-1.7237520 \times 10^{-4}, 8.1394037 \times 10^{-19})$
$A_5 = (8.502311 \times 10^{-5}, -2.0991458 \times 10^{-19})$
$A_6 = (-5.1531855 \times 10^{-5}, -3.2732869 \times 10^{-19})$
$A_7 = (3.1820187 \times 10^{-5}, -5.3546784 \times 10^{-19})$
$A_8 = (-2.2444078 \times 10^{-5}, -4.5320629 \times 10^{-19})$
$A_9 = (1.54729739 \times 10^{-5}, -4.8304523 \times 10^{-19})$

3. Numerical Analysis

Eigenvalues are calculated when the opening angle of the notch $2(\pi-b)=90^\circ$. Firstly, characteristic equation (Eq.(10)) is solved by the Newton-Raphson method. Infinite number of complex eigenvalues exist. Calculated eigenvalues are listed in Table1. First eigenvalue is real and the rest of eigenvalues are complex. It is certified that the stress free boundary conditions ($\sigma_{\theta}=\tau_{r\theta}=0$ at $\theta=\pm b$) are satisfied with the calculated eigenvalues numerically. Using the Schmidt method the distributed load on the circumferential edge (Eq.(3), "Original" in Fig.2) are expanded into the orthogonal function series (Eq.(13), "Expanded" in Fig.2). The calculation error have the maximum value at $\theta=0$ and the error is 4.8%. By using the Schmidt method unknown constants, A_n , are calculated and listed in Table1. These constants are real. Stress distributions are shown in Fig.3. The large tensile stresses occur at $\theta=0$ for σ_{θ} and $\theta=\pm 135^\circ$ for σ_r . Comparing Fig.2(a) ($\frac{\sigma_r}{p_o} = 0$ at $\theta=0$) and Fig.3 ($\frac{\sigma_r}{p_o} \cong 0.6$ at $\theta=0$) it is cleared that the bi-axial stress field is developed due to the constraint effect of the notch.

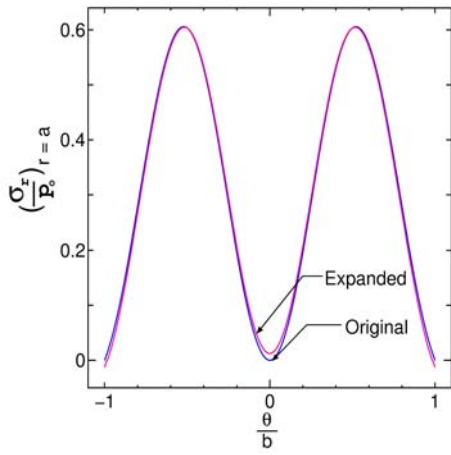
To calculate the stresses distribution in the V-shape notched disk under distributed load we propose following relationships:

$$\sigma_r = p_o \sum_{n=0}^{n=k} A_n W_{rn} r^{\lambda_n - 1}, \quad (19)$$

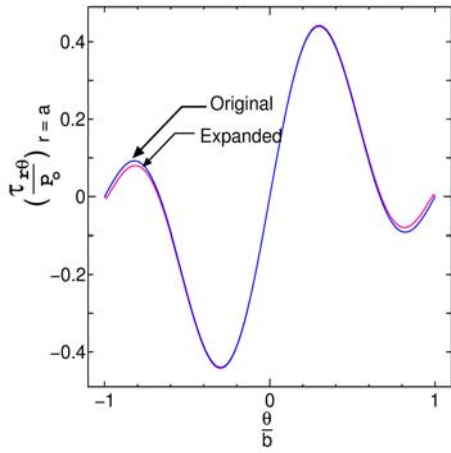
$$\sigma_{\theta} = p_o \sum_{n=0}^{n=k} A_n W_{\theta n} r^{\lambda_n - 1}, \quad (20)$$

$$\tau_{r\theta} = p_o \sum_{n=0}^{n=k} A_n W_{r\theta n} r^{\lambda_n - 1}. \quad (21)$$

$$\begin{aligned} W_{\theta n} &= -\lambda_n [(\lambda_n + 1) \cos(\lambda_n + 1)\theta \\ &\quad + R_n \left\{ \frac{\lambda_n - \kappa}{2} \cos(\lambda_n + 1)\theta \right. \\ &\quad \left. + \frac{\lambda_n + 1}{2} \cos(\lambda_n - 1)\theta \right\}]. \end{aligned}$$



(a)



(b)

Figure 2: Comparison between external distributed load and its expanded result

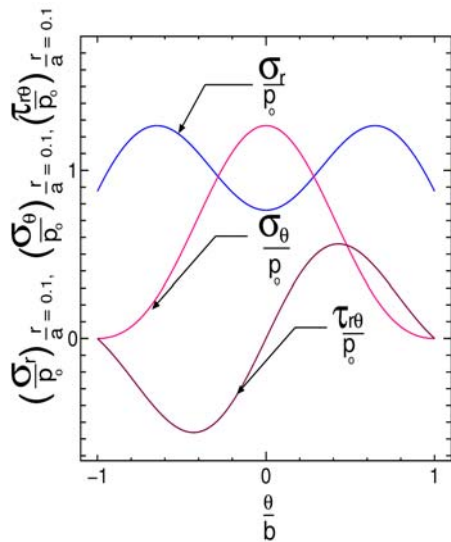


Figure 3: Stress distribution along the circumferential direction

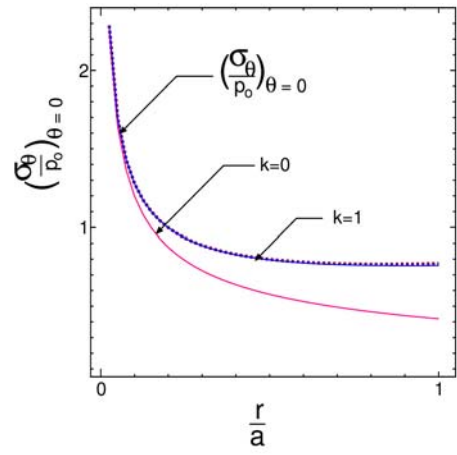
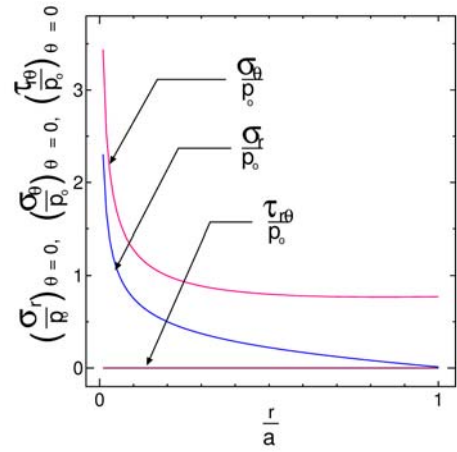
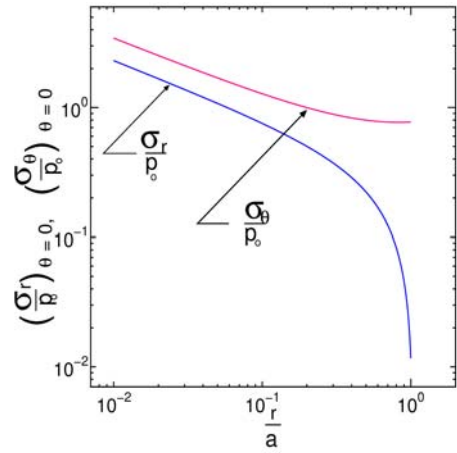


Figure 4: Comparison between exact solution and asymptotic solutions for tangential stress σ_θ distribution along radial direction



(a) Linear plot



(b) log-log plot

Figure 5: Stress distribution along radial direction

W_{rn} and $W_{r\theta n}$ are already given in Eq.(13). Figure 4 shows the comparison of full and asymptotic solutions. In the figure $(\frac{\sigma_\theta}{p_0})_{\theta=0}$ is the full solution ($k \rightarrow \infty$ in Eq.(20)). $k=0$ is the first order asymptotic solution, $k=1$ is the summation of the first and

second order asymptotic solutions. The ranges of applicability of the asymptotic solutions are $\frac{r}{a} \leq 0.01$ for $k = 0$, and $\frac{r}{a} \leq 1$ for $k=1$ with the error of less than 0.1%. Figure 5 illustrates that the summation of the first and second order asymptotic solution gives reasonable approximation for $\sigma_\theta - r$ relation at $\theta = 0$.

Figure 5(a) shows the stress distribution along the radial axis at $\theta = 0$. σ_θ is the maximum stress distribution and $\tau_{r\theta}$ is the minimum stress distribution. Figure 5(b) shows the log-log plot of the stress distribution along the radial axis. Straight line relationships are shown close to the apex of the notch.

4. Comparison with experiment

To compare the calculated result of the difference of principle stresses with experimental result, photoelastic experiments have been done. In analytical model the boundary condition on the circumferential edge (Eq.(3)) is the stress distribution of uniaxial tension, $\sigma_r(\theta) = \frac{1}{2}(1 - \cos 2\theta)$, $\tau_{r\theta}(\theta) = \frac{1}{2} \sin 2\theta$, times $\cos \frac{\pi\theta}{2b}$. $\cos \frac{\pi\theta}{2b}$ is needed for the notch edge stress free condition. This boundary condition in the analytical model is considered to be similar to the stress field around V-shape notch in a strip subjected to uniaxial tension because the remote stress fields for the both models are uniaxial tension. From this reason, in this study, the analytical results about V-shape notched disk are compared with the experimental results of the V-shape notched strip. A specimen shown in Fig.6 which has two V-shape notch(opening angle $2(\pi-b)=90^\circ$) in both sides of the strip were machined out from a epoxy plate. Then this strip was annealed to remove the residual stresses of the material. In annealing process, firstly 1 hour is needed to arise the room temperature to 120°C . Secondly, this temperature was kept for 40 minutes. Thirdly, the temperature is gradually down $10^\circ \text{C} / \text{hr}$ and if the temperature reached to 80°C , the annealing process was stopped. The specimen was set to the photoelastic experiment equipment where the tensile load was applied. For photoelasticity the following relation can be used to determine the difference of principle stresses:

$$\sigma_1 - \sigma_2 = \frac{n}{\alpha d}, \tag{22}$$

where, n is fringe order, α is the photoelastic constant (0.96 mm/kgf for the material used), d is thickness of the specimen. Figure 7 shows the fringe pattern in the specimen around V-shape notch. Figure 8 gives the comparison between the experimental results and the numerical results for σ_r at $\theta = \frac{3}{4}\pi$ (along the notch edge). The distribution characteristics are in good agreement qualitatively.

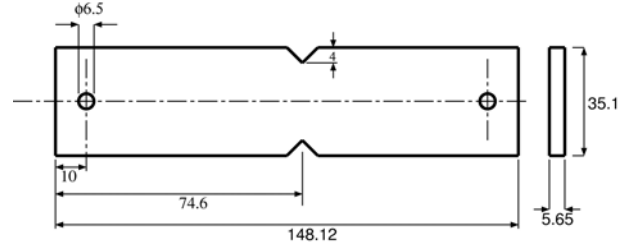
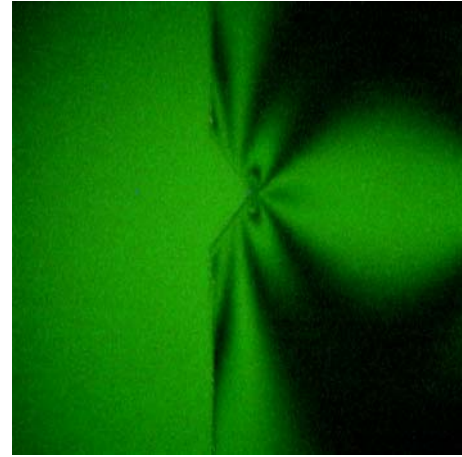
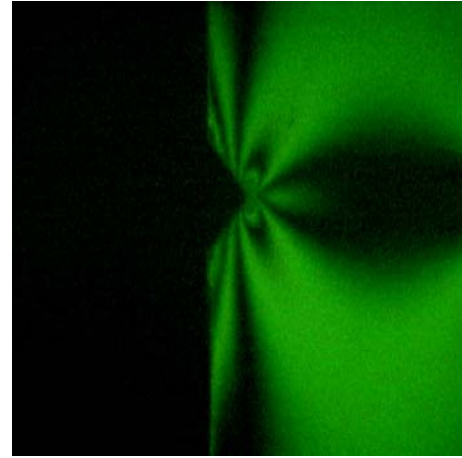


Figure 6: Specimen configuration (unit: mm)



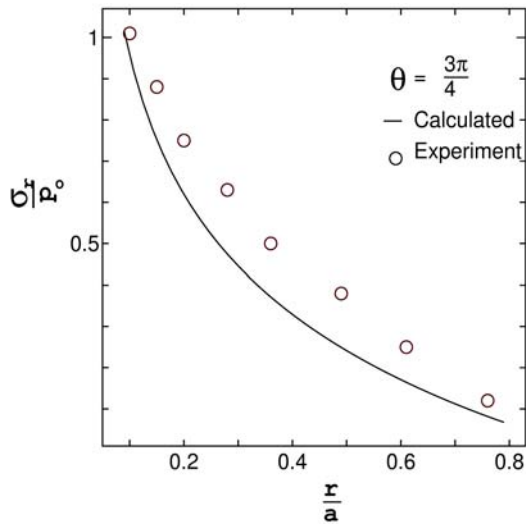
(a) Bright field



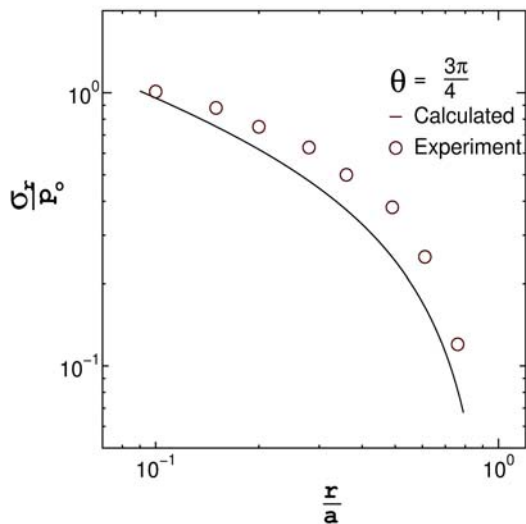
(b) Dark field

Figure 7: Photoelastic experiment result. ($p_o=7.2$ MPa)

The distribution of the difference of principal stresses along the tangential direction are shown in Figure 9. The qualitative agreement (between the calculated results and the experimental results) in tangential direction of the stresses is also verified. Figure 8 and 9 suggest that the result of the present analysis is valid to evaluate the stress distribution around the V-shape notch strip qualitatively.



(a) Linear plot



(b) log-log plot

Figure 8: Comparison between experimental and numerical results along the radial direction

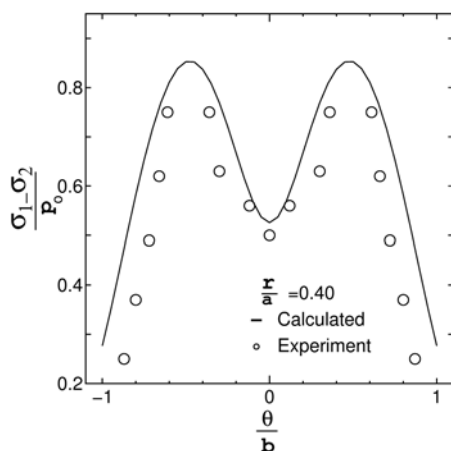


Figure 9: Comparison between experiment and numerical result (tangential distribution)

5. Conclusion

A new method is developed for determining the stress and displacement fields around a sharp V-shape notched disk which is symmetrically loaded on the circumferential edge. Complex eigen function expansion is used to satisfy the stress free condition of the sharp V-shape notch. Boundary condition of the external load applied on the circumferential edge is satisfied with the aid of the Schmidt method. An example of numerical calculation on the stress field is presented and examined. Approximation expressions based on the eigen function expansion are proposed and its validity is confirmed. Finally, the numerical results are compared to photoelastic experiment. Results are summarized as follows;

(1) Infinite number of complex eigenvalues exist. First eigenvalue is real and the rest of eigenvalues are complex. It is certified that the stress free boundary conditions are satisfied with the calculated eigenvalues numerically.

(2) The range of applicability of the asymptotic solutions are $\frac{r}{a} \leq 0.01$ for $k = 0$, and $\frac{r}{a} \leq 1$ for $k=1$ with the error of less than 0.1%. The summation of the first and second order asymptotic solution gives reasonable approximation for $\sigma_\theta - r$ relation at $\theta = 0$.

(3) The qualitative agreement between the analytical results and experimental results in radial and tangential direction of the stresses are verified.

References

- [1] Williams, M. L., "Stress singularities Resulting from various boundary conditions in Angular Corners of Plates in Extension," J. of Appl. Mech. Vol. 19, pp. 526-528 (1952).
- [2] Theocaries, P. S. "Elastic stress intensity factors evaluated by caustics," in Mechanics of Fracture, Vol. 7, ed. G. C. Sih, pp. 189 -252 (1980).
- [3] Theocaries, P. S. and Ioakimidis, N.I., "The V-notch Elastic Half-Plane Problem," Acta Mech. Vol. 32, pp. 125-140 (1979).
- [4] Chen, D.-H. and Nisitanni, H., "Singular Stress Fields near the Tip of a V-notch in a Semi-Infinite Plate," Trans. JSME, Ser. A, Vol. 57, No.538, pp. 128-133 (1991) (in Japanese).
- [5] Mainfalah, M. and Zachary, L. "Mode I and II stress Intensity factors in 90° reentrant corners," Proceedings 1990 SEM spring conf. pp. 446-450 (1990).
- [6] Mainfalah, M. and Zachary, L. "Photoelastic determination of mixed mode stress intensity factors for sharp reentrant corners," Engng. Fracture Mech., Vol. 52, No. 4, pp. 639-645 (1995).
- [7] Kondo, T., Kobayashi, M. and Sekine, H. "Strain Gage Method for determining Stress Intensity of Sharp -Notched Strips," J. Exp. Mech., Vol. 41, pp. 1-7 (2001).

- [8] Prassianakis, J. N. and Theocaries, P. S., "Stress Intensity Factor at V-notched Elastic symmetrically Loaded Plates by the Caustic," J. Phys. D: Appl. Phys., Vol. 13, pp. 1045-1053 (1980).
- [9] Tsuchida, E., Ohno, M. and Kouris, D.A., "Effects of an Inhomogeneous Elliptic Insert on the Elastic Field of an Edge Dislocation," Appl. Phys., A53, pp. 285-291 (1991).
- [10] Morse P. M. and Feshback, H., "Method of Theoretical Physics," part-I, pp. 928-931(1953).